Electronic Supplementary Material (ESI) for Nanoscale.

<Supplementary Information>

Stabilization of a Ga-adlayer structure with the zincblende stacking sequence in the GaN(0 0 0 –1) surface at the nanoscale

Sung Bo Lee,[a,*] Seung Jo Yoo,[b] Kunsu Kim,[a] Yong-Sung Kim,[c,*] Young-Min Kim,[d,e,*] Jin-Gyu Kim,[b] and Heung Nam Han[a]

[a]*Department of Materials Science and Engineering and Research Institute of Advanced Materials (RIAM), Seoul National University, Seoul 08826, Republic of Korea. E-mail: bolee@snu.ac.kr*

[b]*Nano-Bio Electron Microscopy Research Group, Korea Basic Science Institute, Daejeon 34133, Republic of Korea*

[c]*Korea Research Institute of Standards and Science and Department of Nano Science, University of Science and Technology, Daejeon 34113, Republic of Korea. E-mail: kimyongsung@gmail.com*

[d]*Center for Integrated Nanostructure Physics, Institute for Basic Science (IBS), Suwon 16419, Republic of Korea*

[e]*Department of Energy Science, Sungkyunkwan University (SKKU), Suwon 16419, Republic of Korea. E-mail: youngmk@skku.edu*

Notes: 7 sections

Figures: S1–S10

References: 1–13

Surface polarity determined by convergent beam electron diffraction (CBED). The polarity of the surface was determined by CBED,[1] which was performed along the <0 1 –1 0> direction of the specimen. The <0 1 –1 0> axis was chosen, since the (0 0 0 2) diffraction disks are well-spaced from the surrounding disks along the zone axis.[2] As shown in Fig. S1(c), the experimental CBED pattern (left) and a simulated <0 1 –1 0> CBED pattern, which is calculated for a specimen thickness of 110 nm, correctly fits each other, indicating that the surface normal direction is [0 0 0 –1].

High-resolution transmission electron microscopy (HRTEM) image simulation. The image simulation of the HRTEM images [Fig. S2(b)] was implemented by using the JEMS software[3] at an overfocus of 45 nm and a specimen thickness of 5 nm. It was based on the supercell determined by the ab initio calculation (Fig. 4). For the simulation, we considered microscope parameters of the ARM, such as the acceleration voltage (1250 keV), spherical aberration (2.65 mm), chromatic aberration (4.1 mm), and defocus spread (8 nm).

Figure S2(a) is the same as Fig. 1a. In Fig. S2(b), a white boxed area in Fig. S1(a) is overlaid with a simulated HRTEM image, and the corresponding atomic model (green for Ga and red for N), which was adapted from Fig. 4(d). Fig. S2(b) indicates that, under the imaging condition of the present study, Ga atoms appear white. As noted above, the ab initio

calculations predict an inward relaxation along the surface layer. Actually, such an inward relaxation is experimentally confirmed [Fig. S2(b)]. The atomic positions in the surface layer coincide with those calculated.

Rare observation of atomic attachments on the surface leading to the ZB stacking sequence in the surface layers. Even atomic attachments on the surface are rarely observed during annealing (Fig. S4). At first the surface layers follow the WZ stacking sequence. However, as annealing progresses, atoms are sitting on ***C*** sites (indicated by an arrow in the panel for 1.1 s), revealing the ZB stacking sequence in the topmost three Ga layers. After prolonged annealing, the attached layer eventually disappears.

GaN and electron-beam damage. Since the specimen was irradiated by the high-energy electrons during annealing, the layer-by-layer decomposition might be influenced by damage due to inelastic (electron–electron) scattering or damage due to elastic (electron–nucleus) scattering.[1,4] The former damage includes radiolysis and electron-beam heating. The latter includes knock-on damage and electron-beam sputtering. For damage due to inelastic scattering, the temperature rise by beam heating is calculated to be negligible (Δ T = ~0.01 K), because of the high thermal conductivity of GaN (230 W m^{-1} K^{-1} at 300 K[5]). Radiolysis indicates chemical bond breaking through inelastic scattering (ionization).

For GaN, radiolysis effect is not significant as compared with atomic displacement due to elastic scattering, such as Knock-on damage and sputtering, because of its relatively high electrical conductivity. Electronic excitations of atomic electrons by a beam of electrons must remain long enough to cause atomic displacement by radiolysis, for which the relaxation time

of excited electrons should be longer than 1 picosecond (ps).[6] The relaxation time is approximated by $\tau = \varepsilon_0 \varepsilon_r \rho_R$,[6] where ε_0, ε_r, and ρ_R are the vacuum permittivity, the relative permittivity, and the resistivity of a material. However, for conducting materials, whose resistivity is less than 10^{-3}–10^{-4} Ω m, electronic excitations are too short to cause atomic displacement and damage due to inelastic scattering would be minor, because the excitations can be rapidly delocalized by the conduction electrons.[6] For undoped GaN, the resistivity is determined to be ~10^{-3} Ω m (for undoped GaN layer on sapphire by vapor phase technique)[7,8] and the relative permittivity is 8.9, producing a relaxation time of 7.9×10^{-2} ps, too short to cause atomic displacement. Thus, both the bulk and the surface of GaN are not likely to be damaged by radiolysis.

For damage due to elastic scattering, knock-on damage means the direct displacement of atoms *within* a specimen, which occurs only above the threshold incident electron energy. If atomic displacement occurs at the surface of a specimen, it is termed sputtering, which can occur at voltages of 50 % or less of the knock-on threshold.[1,4] According to Look *et al.*,[9] the displacement energies of Ga and N in GaN are 20.5 eV and 10.8 eV, respectively. These values correspond to the *threshold* energies for displacement[4] of 0.45 MeV for Ga and 0.065 MeV for N. Since the threshold energy values are lower than the incident energy of 1.25 MeV, Ga and N atoms in the crystal lattice and in the surface will be easily displaced by the incident electrons.

However, the concept of knock-on damage does not apply to the structural changes in the surface, because it deals with the atomic displacement within a specimen. Moreover, electron energy loss spectroscopy (EELS) in our previous study[10] did not reveal any indication of point defect formation by knock-on damage during observation at 500ºC, which is attributed to an annealing effect at the high temperature.[10] Instead, electron-beam sputtering can facilitate a

layer-by-layer decomposition, as shown in the present study. Taken together, it is concluded that the decomposition occurs by the thermal effect in combination with electron-beam sputtering.

Relation between the slab size, *D*, and the geometric integer, *m*. The geometric relation of $D = 0.28\ (2m + 2)$ (in nm) is schematically described in Fig. S6.

Justification for and generalization of the hexagonal slab model. In order to see the dependence of the stability on the slab model, we construct two triangular slab models in addition to the hexagonal slab model. One triangular slab model denoted N-edge [Fig. S7(b)] has the N-terminated edges on the triangular GaN(0 0 0 –1) surface. The other one denoted Ga-edge [Fig. S7(c)] has the Ga-terminated edges on the surface. The stability of the Ga-adlayer in WZ stack is compared with that in ZB stack with these different slab models. Fig. S7 shows the Ga-adlayer in WZ stack, and Fig. S8 shows that in ZB stack.

The calculated surface energies relative to the ideal cleavage GaN(0 0 0 –1) surface are shown in Fig. S9, where we used the data of Ga-rich limit condition. This is because, for the GaN(0 0 0 –1) N-polar surface, the WZ 1 × 1 Ga adlayer structure is predicted to be stable against the unreconstructed, as-cleaved surface under Ga-rich conditions.[11,12] For the Ga-edge triangular slab, the Ga-adlayer in WZ stack is found to be more stable than that in ZB stack, as for the infinite surface. On the other hand, for the N-edge triangular slab, the Ga-adlayer in WZ stack is less stable than that in ZB stack, as for the finite size hexagonal slab (m = 1–6). The two surface energies calculated for the Ga-edge and N-edge triagular slabs (m = 3) are averaged and the surface energies are indicated in Fig. S9. The averaged surface energies of the Ga-edge

and N-edge triangular slabs are close to those for the m = 3 hexagonal slab, which shows that the ZB stack is more stable than the WZ stack.

The N-edge of the GaN(0 0 0 –1) surface plays the role of stabilizing the ZB stack of the Ga-adlayer. The Ga-edge destabilizes the ZB stack. The 3-fold N atoms at the N-edge in the WZ stack Ga-adlayer is stabilized into the 4-fold N atoms at the N-edge in the ZB stack Ga-adlayer reconstruction. Since the energy gain from the N-edge ZB reconstruction is larger than the energy loss from the Ga-edge, in the hexagonal slab, the Ga-adlayer is stabilized in ZB stack.

Thus, the stabilization of the ZB stack Ga-adlayer reconstruction on the GaN(0 0 0 –1) surface is not general for any kinds of finite-size surface, but for the finite-size surfaces having the N-edges, such as the hexagonal surfaces and the N-edge triangular surfaces.

Since the {1 0 –1 0} non-polar surfaces are the most stable among the WZ GaN surfaces (except for the far Ga-rich condition),[13] WZ GaN nanostructures preferentially have the {1 0 –1 0} surfaces to the most extent. It results in the preferential growth in the polar direction with the non-polar {1 0 –1 0} sidewall facets. This is the reason why we adopt the hexagonal slab model.

The contribution from the N-edge between the {1 0 –1 0} surfaces (the sidewall facet) and the (0 0 0 –1) N-polar surface (the top facet) stabilizes the Ga-adlayer reconstruction in ZB stack. The electron counting model is suitable only for semiconducting surfaces that have a finite band gap. Since the Ga-adlayer reconstruction structure, which is stable in Ga-rich condition, is metallic, the electron counting model cannot be applied.

Note added for the first-principles calculations. The relative surface energies for both the

WZ and ZB 1 × 1 Ga-adlayer reconstructions under (a) the Ga-rich and (b) N-rich limit conditions are extracted from Fig. 5 and plotted as a function of the surface size (here, *m*) in Fig. S10. Fig. S10 convincingly demonstrates that, for the infinite surface, the WZ 1 × 1 Ga adlayer is predicted to be more stable than the ZB 1 × 1 Ga adlayer. However, as the surface size decreases, the ZB 1 × 1 Ga adlayer becomes stabilized against the WZ 1 × 1 Ga adlayer, in agreement with the HRTEM observations.

References

1 D. B. Williams and C. B. Carter, *Transmission electron microscopy* (Plenum, New York, 1996).

2 L. T. Romano, J. E. Northrup, and M. A. O'Keefe, *Appl. Phys. Lett.* 1996, **69**, 2394.

3 P. A. Stadelmann, *Ultramicroscopy* 1987, **21**, 131.

4 R. F. Egerton, P. Li, and M. Malac, *Micron* 2004, **35**, 399.

5 G. A. Slack, L. J. Schowalter, D. Morelli and J. A. Freitas Jr., *J. Cryst. Growth* 2002, **246**, 287.

6 N. Jiang, *Rep. Prog. Phys.* 2016, **79**, 1.

7 M. Ilegems, *J. Cryst. Growth* 1972, **13/14**, 360.

8 R. K. Crouch, W. J. Debnam and A. L. Fripp, *J. Mater. Sci.* 1978, **13**, 2358.

9 D. C. Look, D. C. Reynolds, J. W. Hemsky, J. R. Sizelove, R. L. Jones and R. J. Molnar, *Phys. Rev. Lett.* 1997, **79**, 2273.

10 S. B. Lee, S. J. Yoo, Y.-M. Kim, J.-G. Kim and H. N. Han, *Sci. Rep.* 2016, **6**, 26493.

11 A. R. Smith, R. M. Feenstra, D. W. Greve, J. Neugebauer and J. E. Northrup, *Phys. Rev. Lett.* 1997, **79**, 3934–3937.

12 A. R. Smith, R. M. Feenstra, D. W. Greve, M. S. Shin, M. Sikowronski, J. Neugebauer and J. E. Northrup, *J. Vac. Sci. Technol.* 1998, **16**, 2242–2249.

13 C. E. Dreyer, A. Janotti and C. G. Van de Walle, *Phys. Rev. B* 2014, **89**, 081305(R).

Figure legends

Fig. S1 Crystallographic orientation of the GaN epitaxial layer deposited on the α-Al_2O_3 single crystal substrate and determination of the surface polarity by CBED. (a) Scanning electron microscopy image of an FIB lamella. (b) Cross-section TEM image of the GaN layer examined. (c) CBED patterns taken along the <0 1 –1 0> direction of the specimen. Left: the experimental pattern, right: a simulation for a specimen thickness of 110 nm.

Fig. S2 (a) Same as Fig. 1a, but with a white box drawn on it. (b) Enlarged view of the white boxed area in (a) with overlays of a simulated HRTEM image and the corresponding atomic model (green for Ga and red for N). The atomic model used was adapted from Fig. 4(d) (see the main text).

Fig. S3 Transition in local structure from WZ to ZB GaN characterized by local FFT. (a) Same as Fig. 1(a), but marked with an arrow starting from the bulk. (b) A series of 12 selected local areas along the arrow in (a) to obtain (c) the corresponding FFT patterns.

Fig. S4 Focus of the left part of the surface shown in Fig. 2 (at t = 0 s). This image shows that only the topmost three Ga layers follow the ZB stacking sequence.

Fig. S5 Time sequence of HRTEM images showing atomic attachments on the surface resulting in the ZB stacking sequence in the surface layers. The 0 s image was taken at an annealing time of 72 min at 500ºC. The elapsed time is labeled in the upper right corner of each panel image.

Fig. S6 The geometric relationship between *D* and *m*.

Fig. S7 Ga-adlayer reconstructions in WZ stack on the GaN(0 0 0 –1) N-polar surface for the (a) hexagonal (m = 3), (b) N-edge triangular, and (c) Ga-edge triangular slab models.

Fig. S8 Ga-adlayer reconstructions in ZB stack on the GaN(0 0 0 –1) N-polar surface for the (a) hexagonal (m = 3), (b) N-edge triangular, and (c) Ga-edge triangular slab models.

Fig. S9 The calculated surface energies relative to the ideal cleavage GaN(0 0 0 –1) surface for the m = 1–6 hexagonal slab, infinite slab, the m = 3 Ga-edge triangular slab, the m = 3 N-edge triangular slab, and the average of the Ga-edge and N-edge triagular slabs.

Fig. S10 Relative surface energies of the WZ and ZB 1 × 1 Ga-adlayer reconstructions as a function of the surface size under both the Ga- and N-rich limit conditions. The open square and circle symbols are for (a) the N-rich limit condition and the closed symbols for (b) the Ga-rich limit condition.

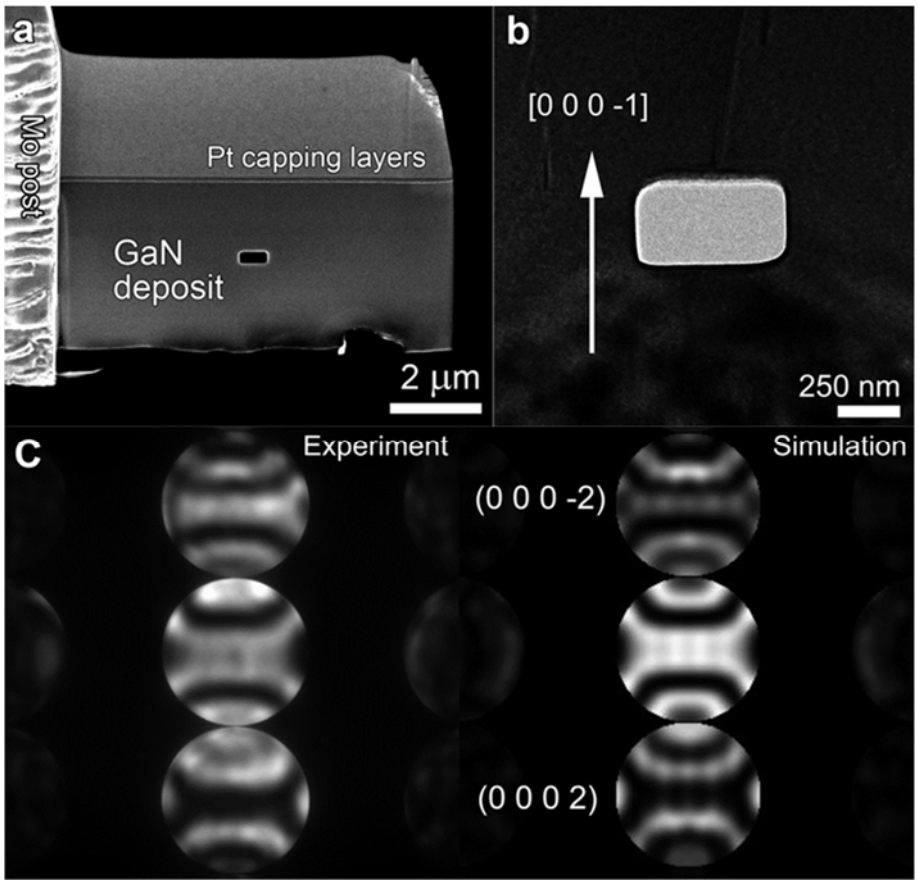

Fig. S1 Crystallographic orientation of the GaN epitaxial layer deposited on the α-Al_2O_3 single crystal substrate and determination of the surface polarity by CBED. (a) Scanning electron microscopy image of an FIB lamella. (b) Cross-section TEM image of the GaN layer examined. (c) CBED patterns taken along the <0 1 –1 0> direction of the specimen. Left: the experimental pattern, right: a simulation for a specimen thickness of 110 nm.

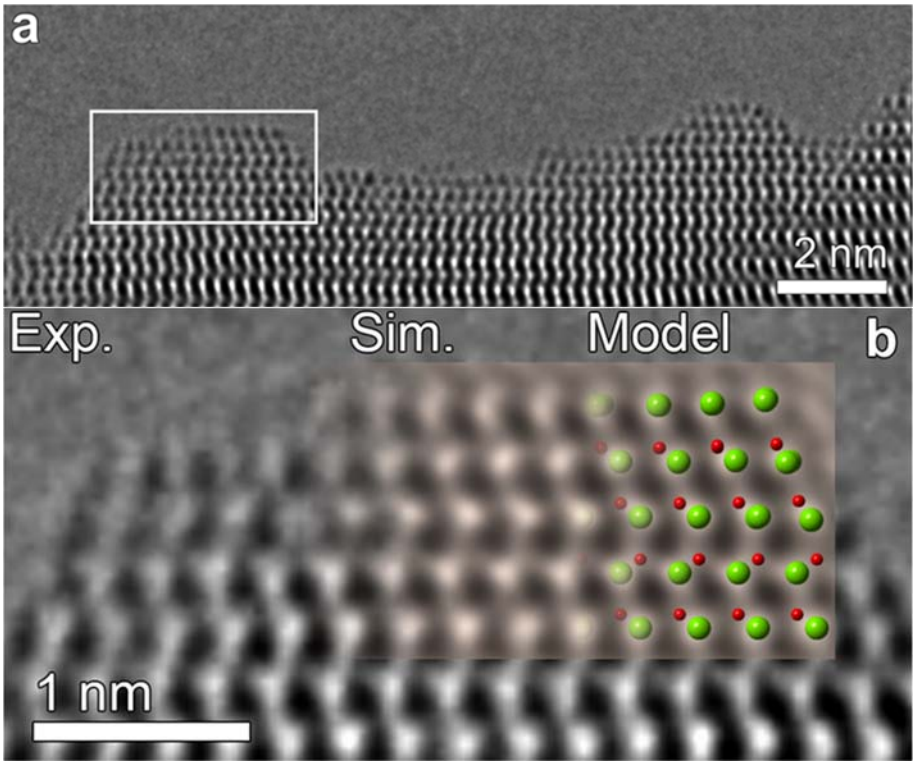

Fig. S2 (a) Same as Fig. 1(a), but with a white box drawn on it. (b) Enlarged view of the white boxed area in (a) with overlays of a simulated HRTEM image and the corresponding atomic model (green for Ga and red for N). The atomic model used was adapted from Fig. 4(d) (see the main text).

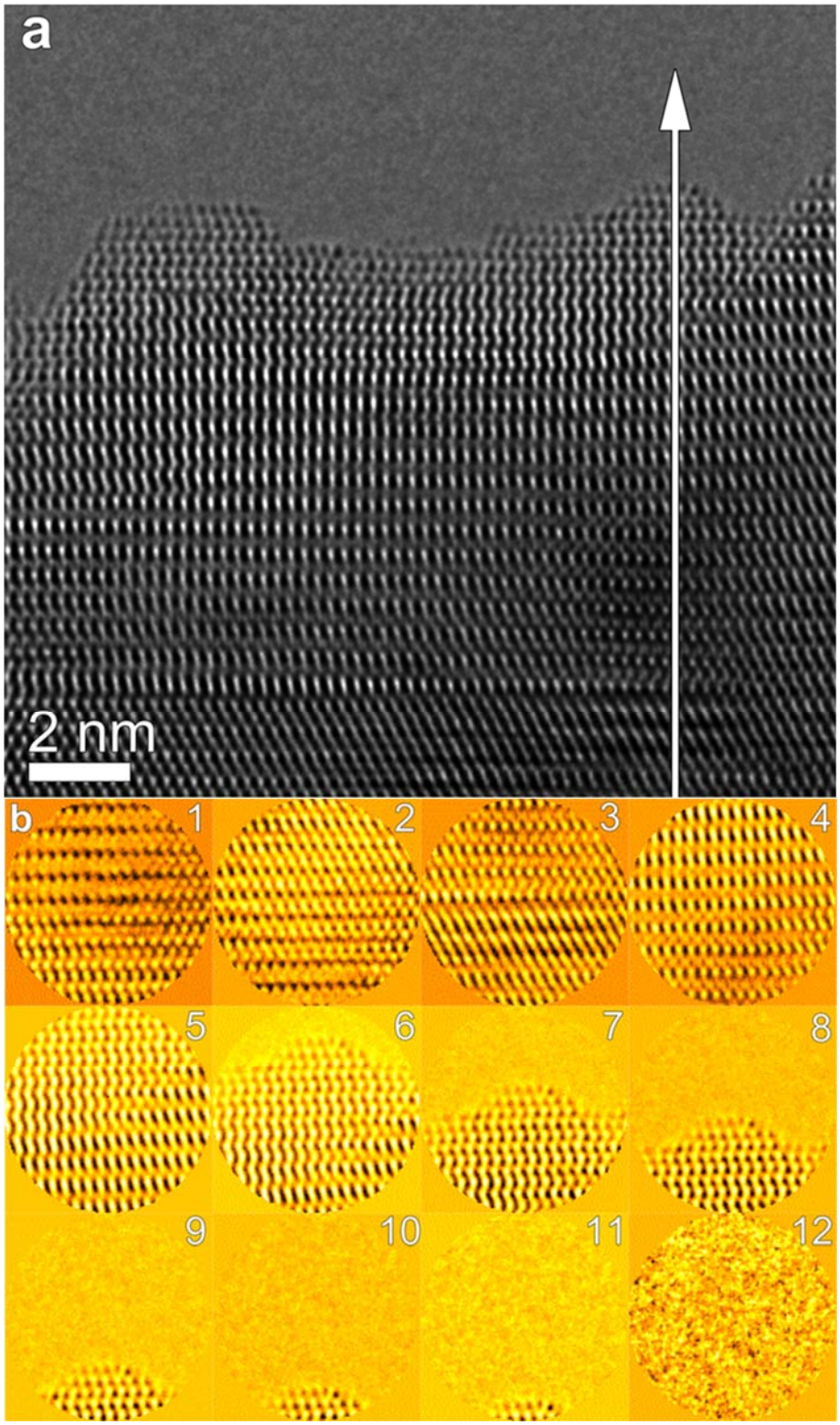

(continued)

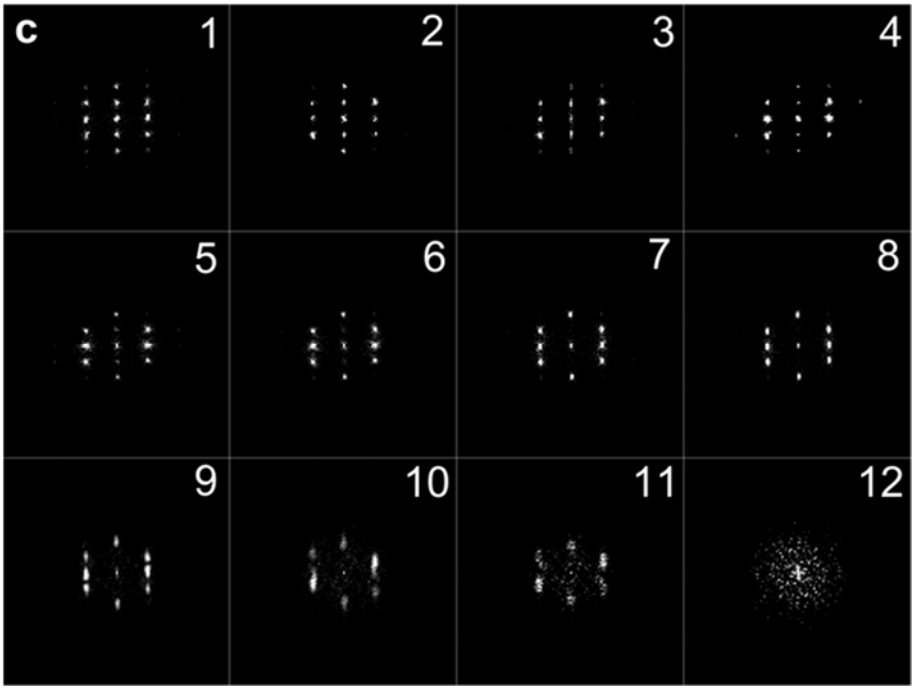

Fig. S3 Transition in local structure from WZ to ZB GaN characterized by local FFT. (a) Same as Fig. 1(a), but marked with an arrow starting from the bulk. (b) A series of 12 selected local areas along the arrow in (a) to obtain (c) the corresponding FFT patterns.

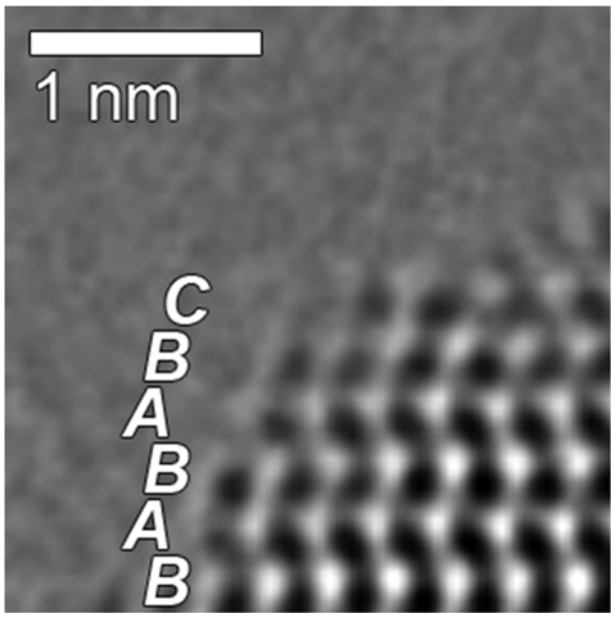

Fig. S4 Focus of the left part of the surface shown in Fig. 2 (at $t = 0$ s). This image shows that only the topmost three Ga layers follow the ZB stacking sequence.

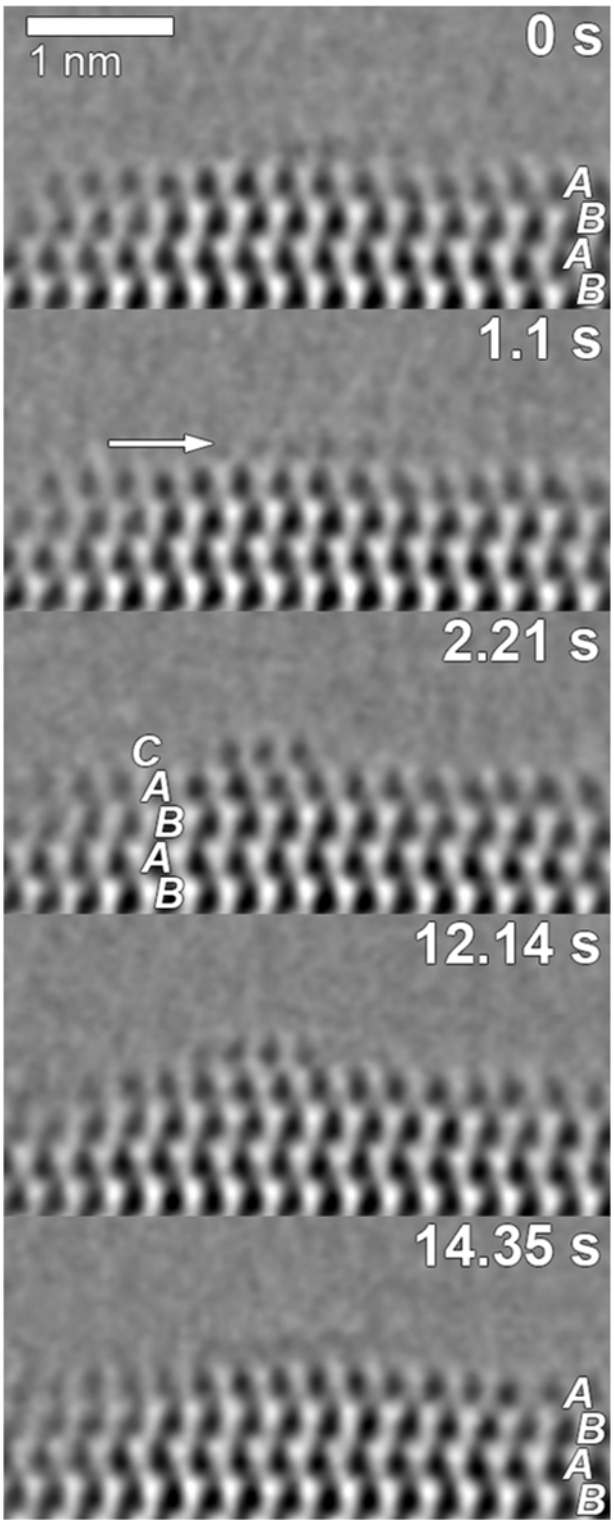

Fig. S5 Time sequence of HRTEM images showing atomic attachments on the surface resulting in the ZB stacking sequence in the surface layers. The 0 s image was taken at an annealing time of 72 min at 500°C. The elapsed time is labeled in the upper right corner of each panel image.

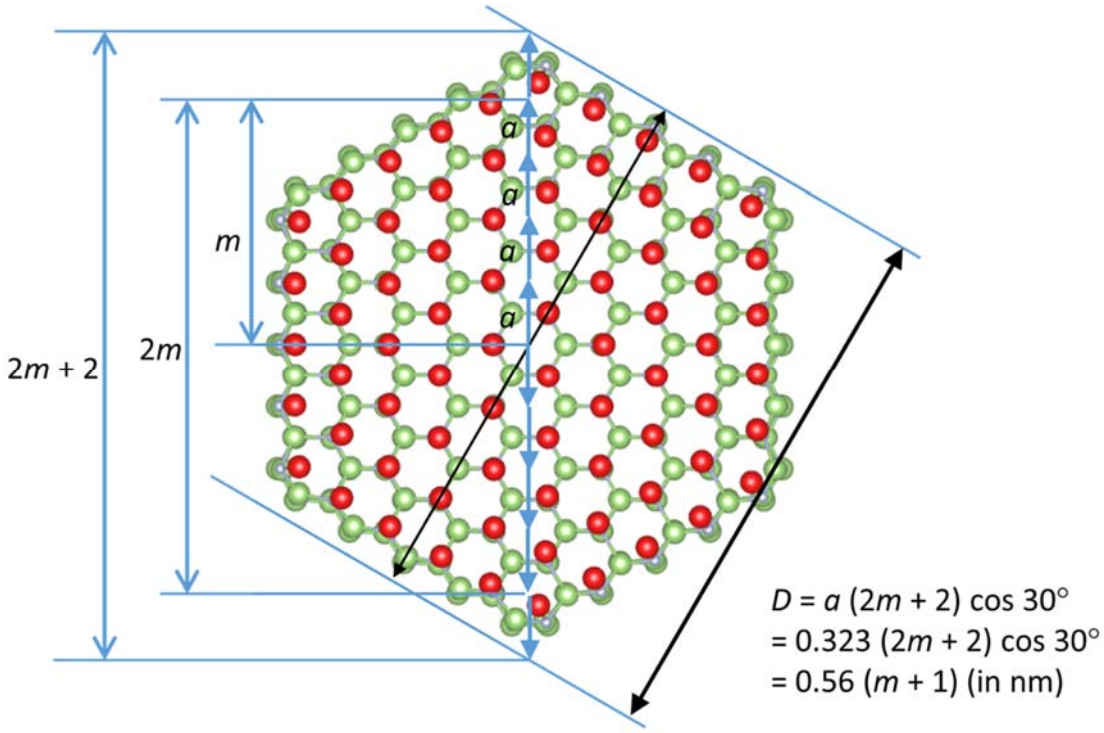

Fig. S6 The geometric relationship between *D* and *m*.

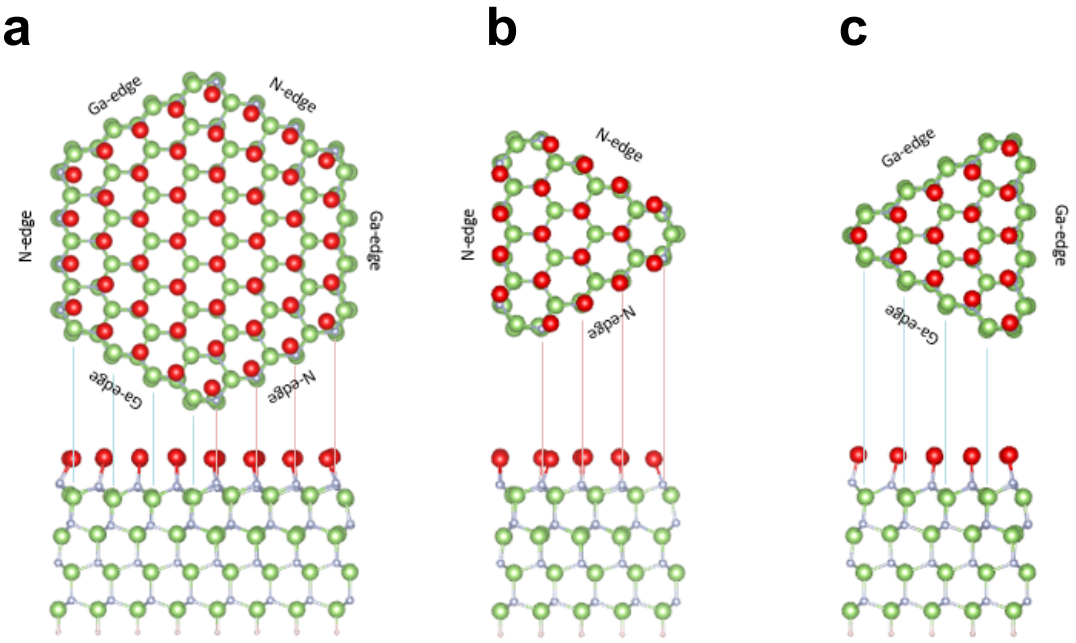

Fig. S7 Ga-adlayer reconstructions in WZ stack on the GaN(0 0 0 –1) N-polar surface for the (a) hexagonal (m = 3), (b) N-edge triangular, and (c) Ga-edge triangular slab models.

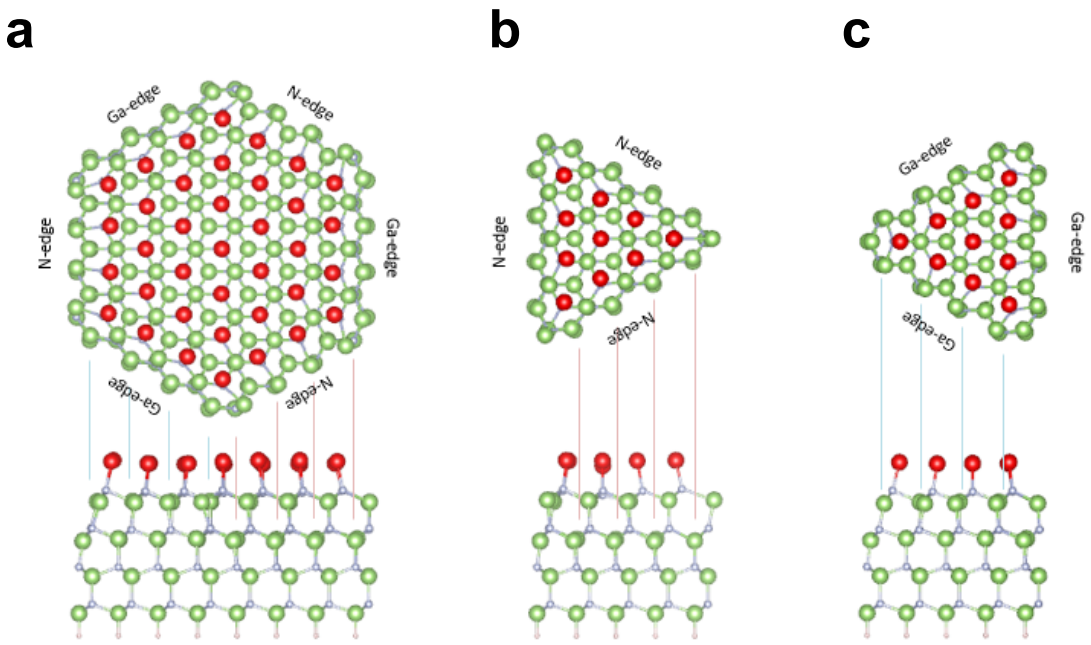

Fig. S8 Ga-adlayer reconstructions in ZB stack on the GaN(0 0 0 –1) N-polar surface for the (a) hexagonal (m = 3), (b) N-edge triangular, and (c) Ga-edge triangular slab models.

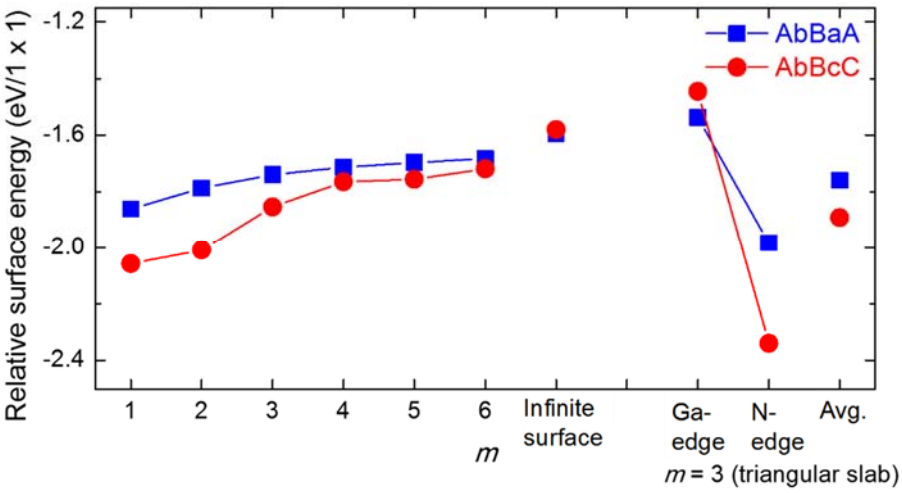

Fig. S9 The calculated surface energies relative to the ideal cleavage GaN(0 0 0 –1) surface for the m = 1–6 hexagonal slab, infinite slab, the m = 3 Ga-edge triangular slab, the m = 3 N-edge triangular slab, and the average of the Ga-edge and N-edge triagular slabs.

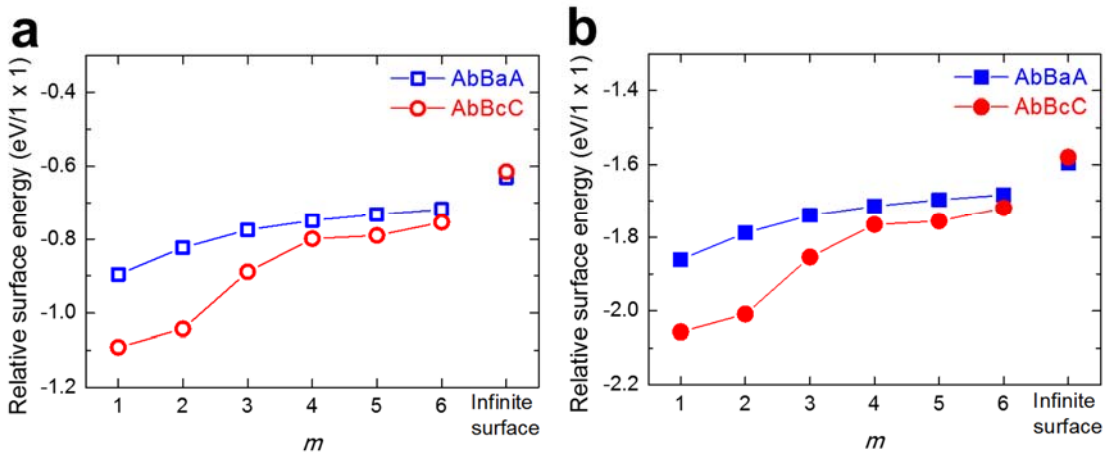

Fig. S10 Relative surface energies of the WZ and ZB 1 × 1 Ga-adlayer reconstructions as a function of the surface size under both the Ga- and N-rich limit conditions. The open square and circle symbols are for (a) the N-rich limit condition and the closed symbols for (b) the Ga-rich limit condition.